Electronic Supplementary Information for

Highly Porous Nitrogen-Doped Carbon Superstructure Derived from the Intramolecular Cyclization-Induced Crystallization-Driven Self-Assembly of a Poly(amic acid)

Hui Sun[*a], Xiao Li[a], Kai Jin[a], Xiaoyong Lai[*a] and Jianzhong Du[*b]

[a]State Key Laboratory of High-efficiency Coal Utilization and Green Chemical Engineering, Ningxia University, Yinchuan 750021, China E-mail: sunhui@nxu.edu.cn, xylai@nxu.edu.cn.

[b]School of Materials Science and Engineering, Tongji University, Shanghai 201804, China E-mail: jzdu@tongji.edu.cn.
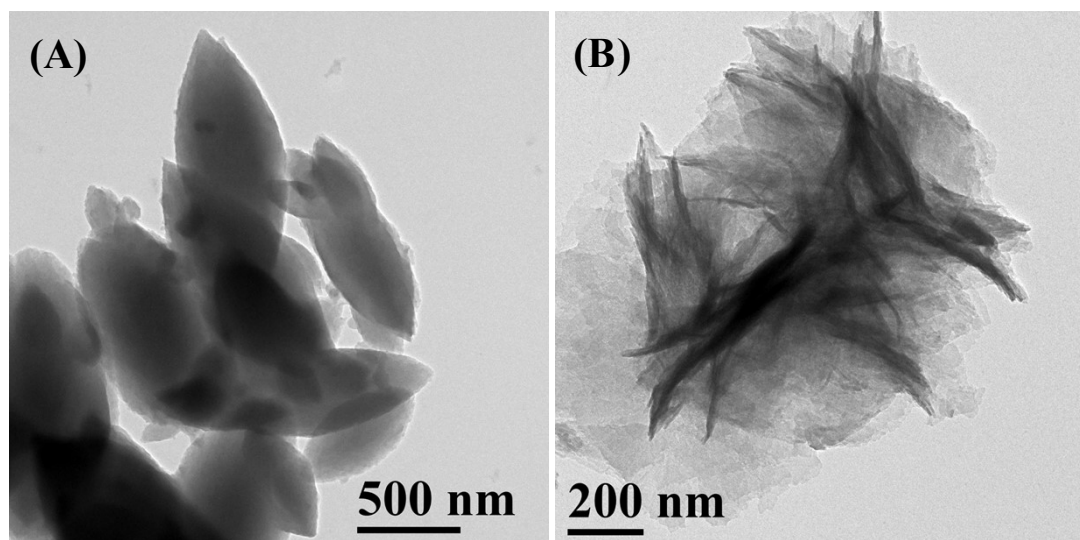
1. Schemes and Figures

Fig. S1. Nano-objects with various morphologies prepared from ICI-CDSA of PAA. (A) PAA solution in DMF incubated at 153 °C for 10 min and (B) PAA solution solvothermal treated at 140 °C for 24 h.

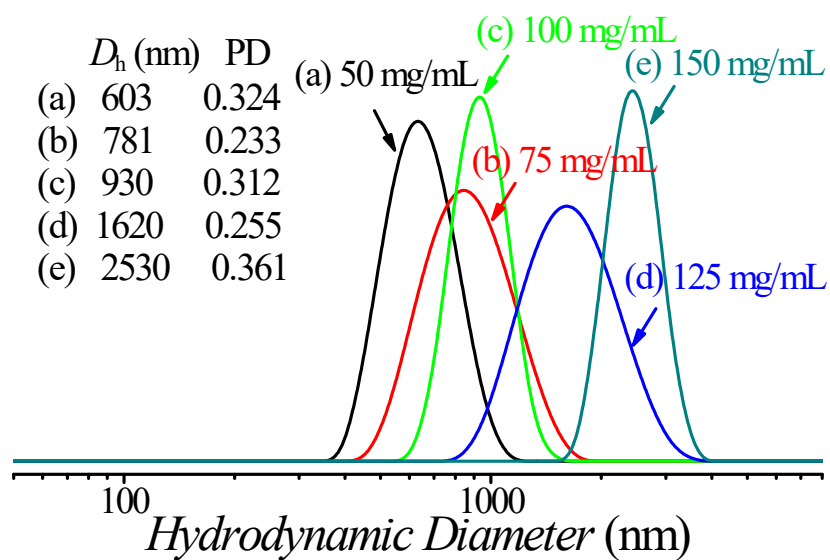| D_h (nm)	PD
(a) 603	0.324
(b) 781	0.233
(c) 930	0.312
(d) 1620	0.255
(e) 2530	0.361

Fig. S2. DLS results of the nano-objects obtained from the ICI-CDSA of PAA in DMF at different concentrations.
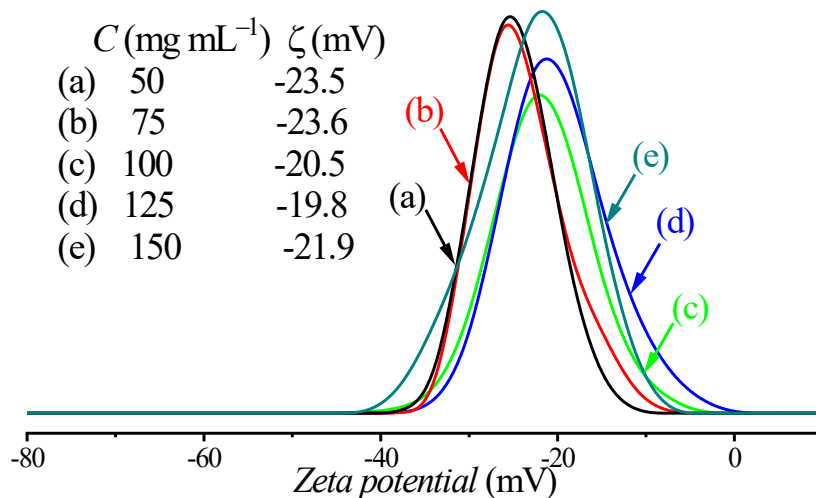
Fig. S3. Zeta potentials of the nano-objects obtained from the ICI-CDSA of PAA in DMF at different concentrations.
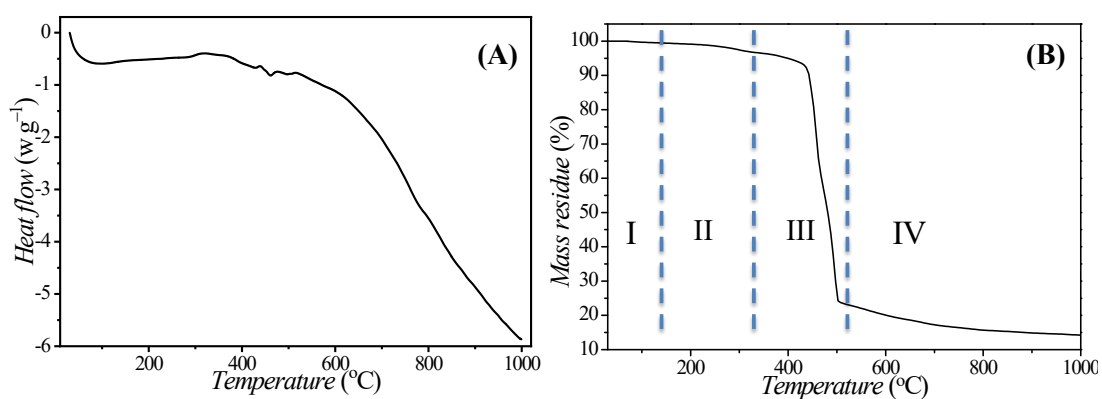

Fig. S4. (A) Differential scanning calorimetry (DSC) and (B) thermogravimetry (TG) results of the hourglass-shaped superstructures pyrolyzed at nitrogen atmosphere.
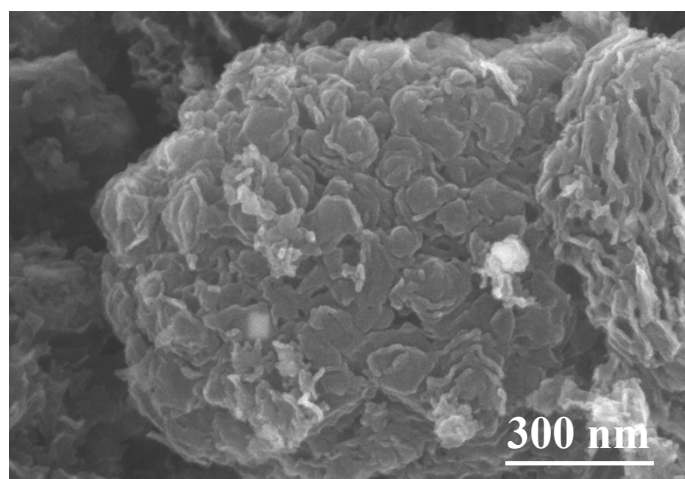
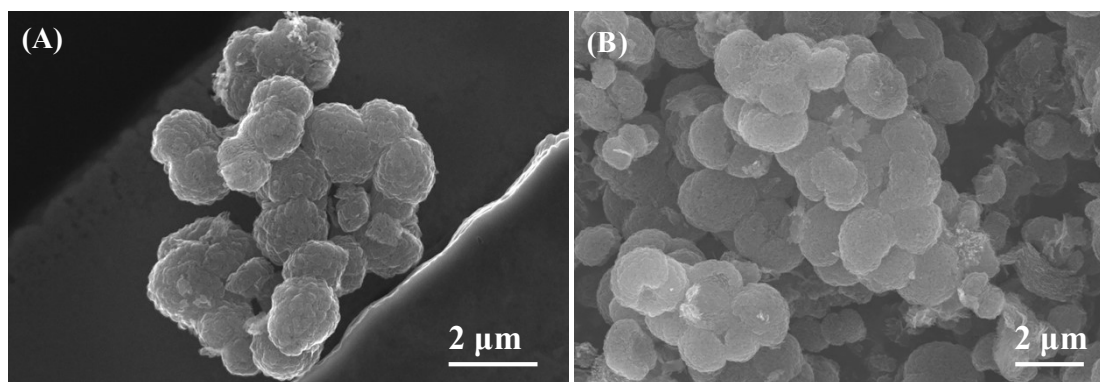Fig. S5. SEM image of N-CSs, confirming that the N-CSs was formed by carbon nanosheets.

Fig. S6. SEM images of N-CSs by the pyrolysis of hourglass-shaped superstructures at (A) 700 and (B) 900 °C.

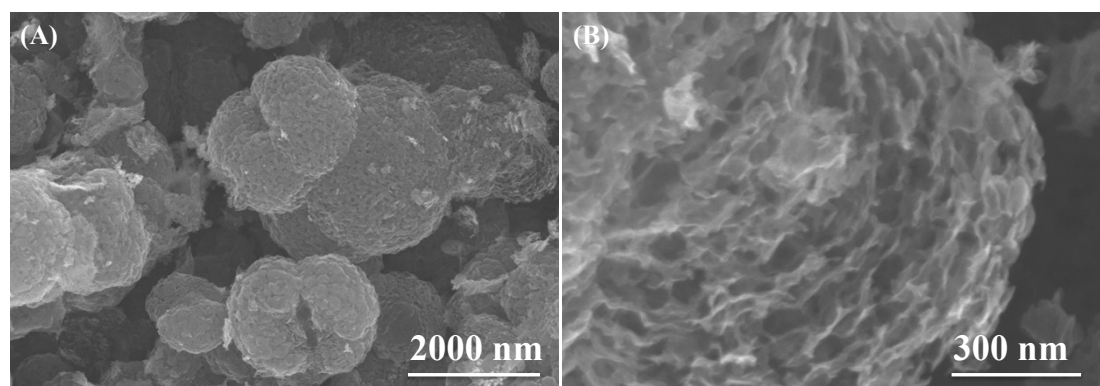Fig. S7. Insight into the inner structure of N-CSs. (A) and (B) SEM images of N-CSs at different magnification.
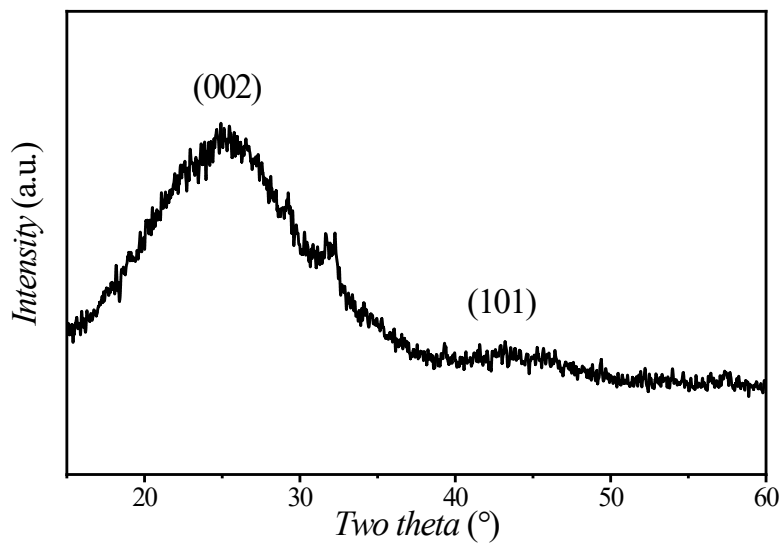
Fig. S8. XRD pattern of N-CSs.

Fig. S9. Raman spectra of N-CSs pyrolized at (A) 700 and (B) 900 °C.
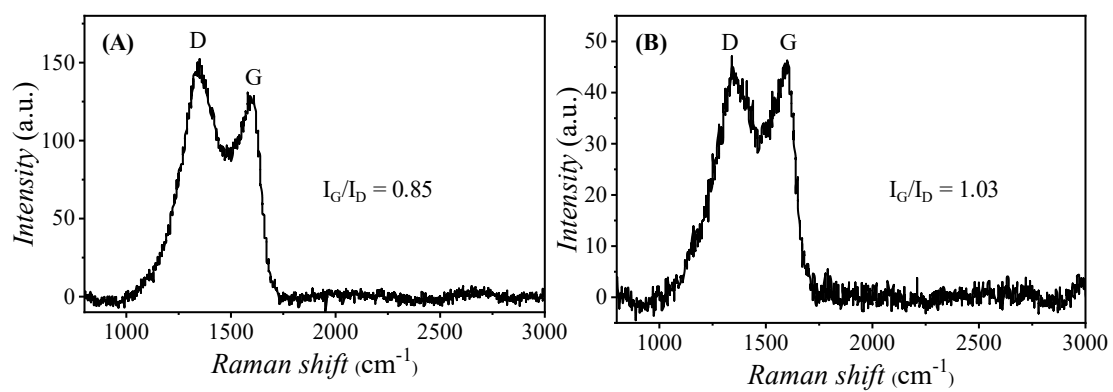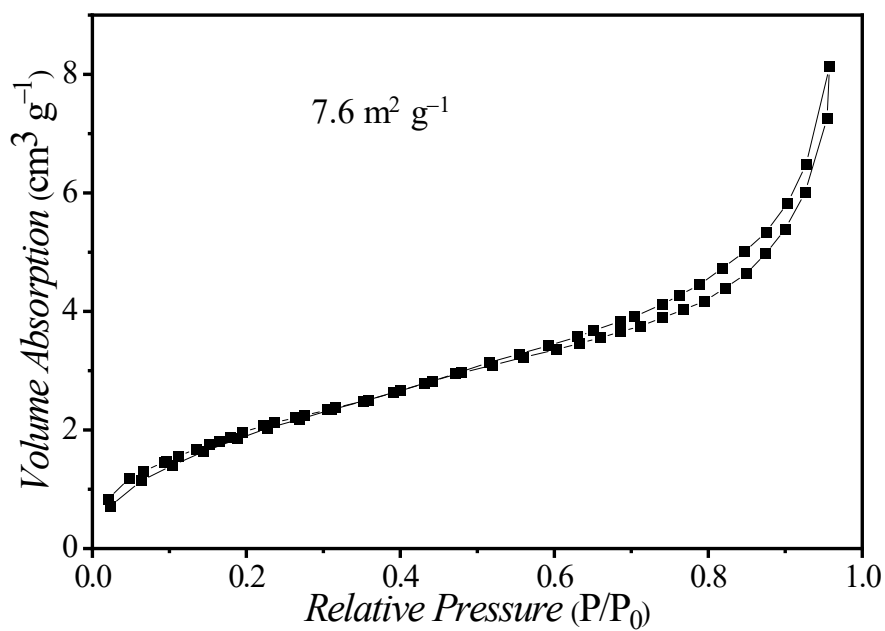
Fig. S10. Nitrogen adsorption/desorption isotherm of hourglass-shaped superstructures.
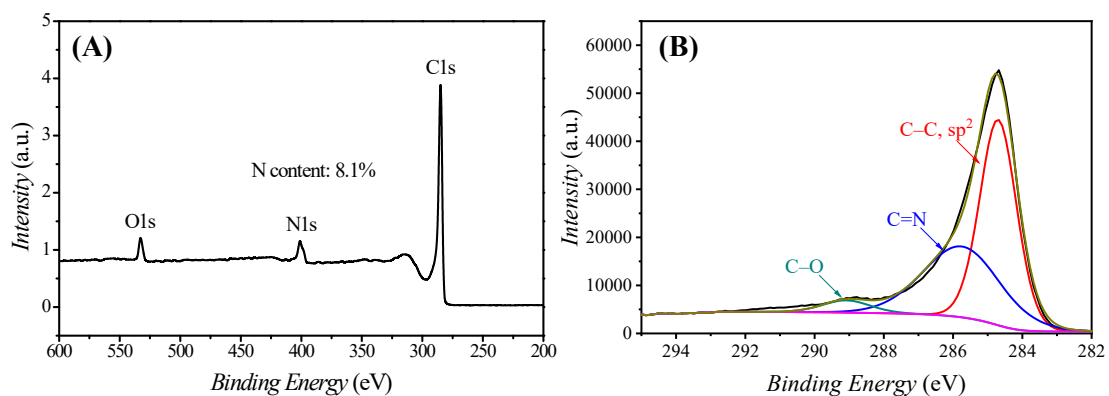

Fig. S11. XPS results of N-CSs. (A) Element contents and (B) high resolution spectrum of carbon.
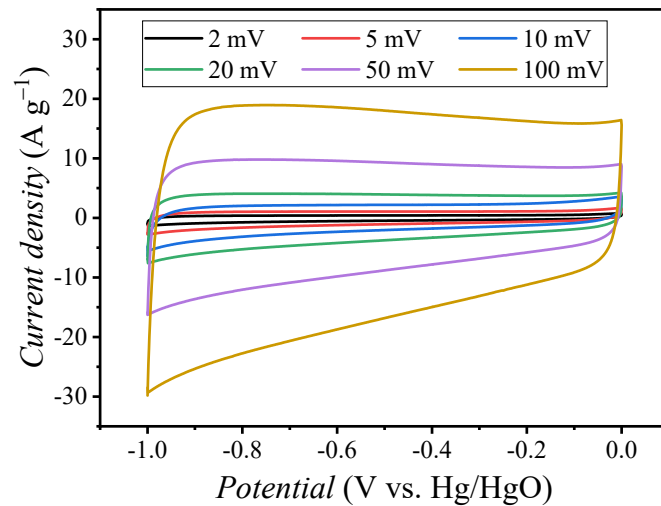
Fig. S12. CV curves of N-CSs at scan rates from 2 to 100 mV s^{-1}.
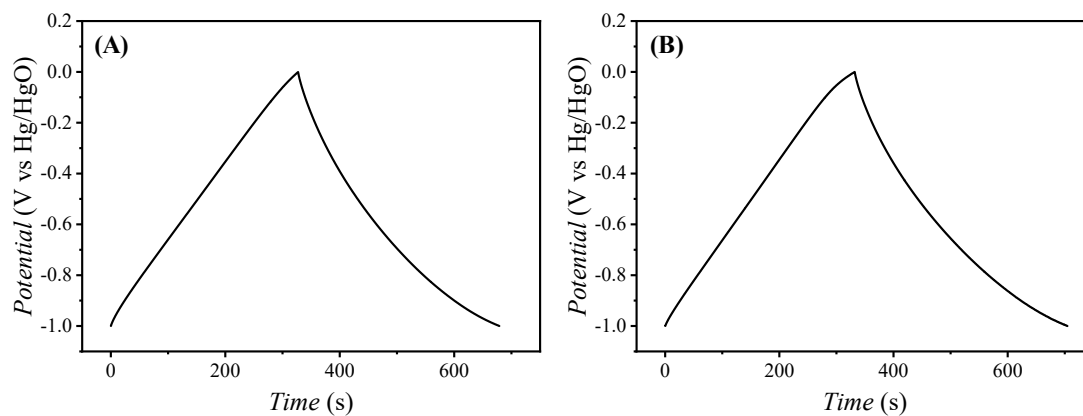
Fig. S13. GC curves of N-CSs pyrolized at (A) 700 and (B) 900 °C at a current density of 0.5 A g^{-1}.
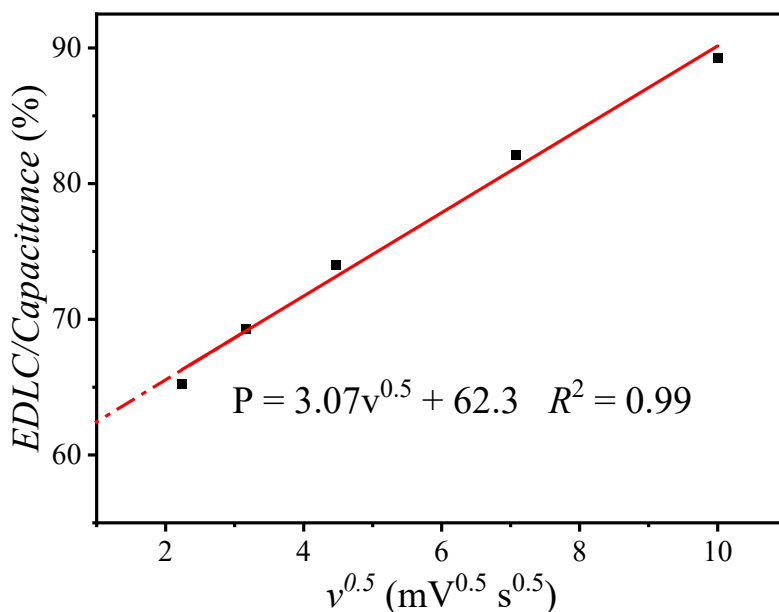
Fig. S14. The relationship between EDLC/capacitance of N-CSs and the square root of scan rate ($v^{0.5}$).

Dunn's method[1]

Dunn's method provides a reliable way to calculate the capacitance contribution of the surface capacitive effects such as the EDL capacitive effects and the diffusion-controlled processes such as pseudocapacitive reactions. At a specific potential, the current density (i) from the CV curves can be expressed as following:

$$i = k_1 v + k_2 v^{0.5} \qquad \text{(I)}$$

Where $k_1 v$ and $k_2 v^{0.5}$ represent the surface capacitive- and diffusion-controlled current contributions, respectively. Divided by $v^{0.5}$ on both sides of equation I, and equation II was obtained.

$$i v^{-0.5} = k_1 v^{0.5} + k_2 \qquad \text{(II)}$$

At a fixed potential, the $i v^{-0.5}$ should have a linear relationship with the square root of scan rates ($v^{0.5}$), and the slope of k_1 and a y-intercept of k_2 are obtained. The $k_1 v$ represents the surface capacitive-

controlled current contribution. At different potentials, a series of k_1 and k_2 could be calculated, and the corresponding surface capacitive-controlled current contributions are obtained.
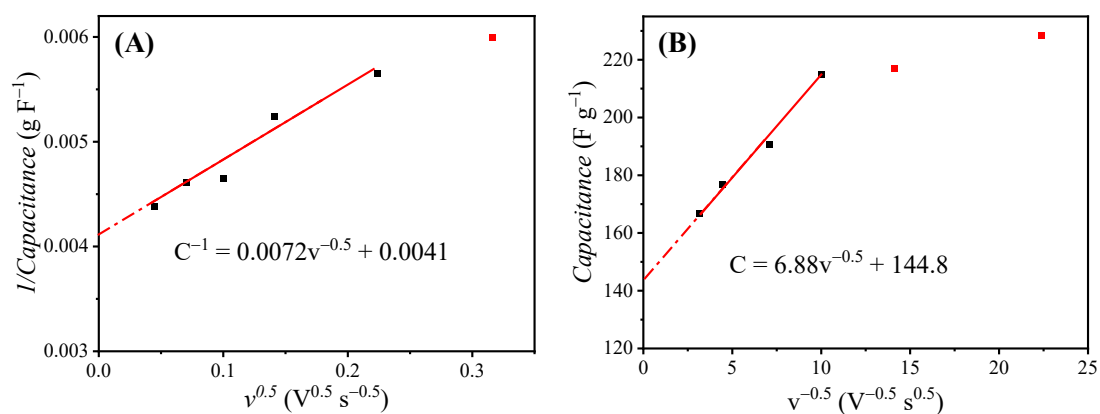
Fig. S15. Capacitance contribution analysis by Trasatti's method. (A) Relationship between the reciprocal of gravimetric capacitance (C^{-1}) and the square root of scan rate ($v^{0.5}$) and (B) relationship between gravimetric capacitance (C) and the reciprocal of square root of scan rate ($v^{-0.5}$).

Trasatti's method [1]

The analysis of contribution of electrochemical double-layer capacitance (EDLC) and pseudocapacitance to the total capacitance by Trasatti's method refers to previous study.[1] Generally, the gravimetric capacitances (C) of N-CSs at different scan rates were calculated according to equation III.

$$C = A/2mv\Delta V \qquad (III)$$

Where A is the area of CV curve, m (g) is the quality of the N-CSs, v is the scan rate ($V\ s^{-1}$), and ΔV is the potential window.

The reciprocal of gravimetric capacitances (C^{-1}) will has a linear relationship with the square root of scan rates ($v^{0.5}$), assuming ion diffusion follows a semi-infinite diffusion pattern, as illustrated in equation IV.

$$C^{-1} = av^{0.5} + b \qquad \text{(IV)}$$

Where b is the reciprocal of total gravimetric capacitance, in other words, the sum of EDLC and pseudocapacitance.

Similarly, the gravimetric capacitances (C^1) will has a linear relationship with the reciprocal of square root of scan rates ($v^{-0.5}$), like equation V.

$$C^1 = a'v^{-0.5} + b' \qquad \text{(V)}$$

Where b' is the EDLC, and the pseudocapacitance could be obtained by subtracting EDLC from total gravimetric capacitance.

Calculation of the utilization of N-6 and N-5 [1-3]

The calculation of the utilization of N-6 and N-5 is based on the results of the calculated pseudocapacitance. It is assumed that the pseudocapacitance is generated from the Faraday reaction of N-6 and N-5. The actual stored electric charge (Q_a (C)) by N-6 and N-5 was calculated to be:

$$Q_a = mC_p\Delta V \qquad \text{(VI)}$$

Where m (g) is the quality of N-CSs, C_p (F g^{-1}) is the pseudocapacitance.

While the theoretically stored electric charge (Q_t) was calculated according to the following equation:

$$Q_t = 2(mW_{N5, N6} F)/M_N \qquad \text{(VII)}$$

Where $W_{N5, N6}$ is the weight percentage of N-5 and N-6 in N-CSs, F is Faraday constant (96485 C mol^{-1}) and M_N is the atomic weight of nitrogen.

Therefore, the utilization of N-5 and N-6 could be calculated by equation VIII.

$$X = Q_a/Q_t \qquad \text{(VIII)}$$

Table S1. Comparison of the structure parameters and electrochemical performances of N-doped carbon materials with literature results.

Electrode Materials	Electrolyte[a]	S_{BET} (m^2 g^{-1})	Pore Width (nm)	C (F g^{-1})[b]	C/ S_{BET} (μF cm^{-2})	References
GO@NMC-3	6 M KOH	255	17	231	90.6	[1]
HCSs	6 M KOH	923	3.9	535	57.2	[4]
NG	6 M KOH	588	11.1	289	49.1	[5]
H-NMC-2.5	6 M KOH	537	14.8	227	42.3	[6]
PA-850	6 M KOH	753	<0.8, 1.5	302	40.1	[7]
PACNP-20	6 M KOH	1317	2.1	362	27.5	[8]
OMCNS	6 M KOH	814	3.1	179	22.3	[9]
N-CSs	6 M KOH	2106	~ 2.3	398	18.9	[10]
MCC-6H	6 M KOH	1797	<3.0, 10-30	301	16.8	[11]
NHPC-800	6 M KOH	1848	1.0-2.0, 2.0-100	260	14.1	[12]
HLPC	6 M KOH	2725	0.7-2.0, 2.0-3.4	342	12.6	[13]
KPAC-800	6 M KOH	2988	2.1, 2.5, 2.5-8.0	238	7.97	[14]
N-CSs	6 M KOH	381	1.0, 3.8, 7.1-38.6	279[c]	76.5	This work

[a]The electrochemical measurements were conducted via a three-electrode system using 6 M KOH as electrolyte. [b]The specific capacitance was obtained at a current density of 0.2 A g^{-1} in previous studies.

[c]The specific capacitance of this work was obtained at a current density of 0.5 A g^{-1}.

2. References

(1) Zhang, L.; Wang, T.; Gao, T.-N.; Xiong, H.; Zhang, R.; Liu, Z.; Song, S.; Dai, S.; Qiao, Z.-A. *CCS Chem.* **2020**, *2*, 870-881.

(2) Wang, Y.; Song, Y.; Xia, Y. *Chem. Soc. Rev.* **2016**, *45*, 5925-5950.

(3) Song, Y.; Li, L.; Wang, Y.; Wang, C.; Guo, Z.; Xia, Y. *Chemphyschem* **2014**, *15*, 2084-2093.

(4) Chen, Z.; Cao, R.; Ge, Y.; Tu, Y.; Xia, Y.; Yang, X. *J. Power Sources* **2017**, *363*, 356-364.

(5) Li, M.; Xue, J. *J. Phys. Chem. C* **2014**, *118*, 2507-2517.

(6) Wei, J.; Zhou, D.; Sun, Z.; Deng, Y.; Xia, Y.; Zhao, D. *Adv. Funct. Mater.* **2013**, *23*, 2322-2328.

(7) Huang, K.; Li, M.; Chen, Z.; Yao, Y.; Yang, X. *Electrochim. Acta* **2015**, *158*, 306-313.

(8) Ma, C.; Li, Y.; Shi, J.; Song, Y.; Liu, L. *Chem. Eng. J.* **2014**, *249*, 216-225.

(9) Yu, X.; Wang, J.-g.; Huang, Z.-H.; Shen, W.; Kang, F. *Electrochem. Commun.* **2013**, *36*, 66-70.

(10) Gao, S.; Chen, Y.; Fan, H.; Wei, X.; Hu, C.; Luo, H.; Qu, L. *J. Mater. Chem. A* **2014**, *2*, 3317-3324.

(11) Wang, T.; Sun, Y.; Zhang, L.; Li, K.; Yi, Y.; Song, S.; Li, M.; Qiao, Z.-A.; Dai, S. *Adv. Mater.* **2019**, *31*, 1807876.

(12) Zhou, J.; Zhang, Z.; Xing, W.; Yu, J.; Han, G.; Si, W.; Zhuo, S. *Electrochim. Acta* **2015**, *153*, 68-75.

(13) Liang, Q.; Ye, L.; Huang, Z.-H.; Xu, Q.; Bai, Y.; Kang, F.; Yang, Q.-H. *Nanoscale* **2014**, *6*, 13831-13837.

(14) Cheng, P.; Gao, S.; Zang, P.; Yang, X.; Bai, Y.; Xu, H.; Liu, Z.; Lei, Z. *Carbon* **2015**, *93*, 315-324.